H_2 CONTROL FOR VARIABLE-SPEED STALL-REGULATED WIND TURBINE

Ronilson Rocha
Peterson Resende
José L. Silvino
Federal University of Minas Gerais - CPDEE
Cx. P. 209 - 30161-970 - Belo Horizonte, MG, Brasil
Marcos V. Bortolus
Federal University of Minas Gerais - DEMEC
Cx. P. 209 - 30161-970 - Belo Horizonte, MG, Brasil

Abstract

This paper presents an H_2 control application for a variable speed stall regulated wind turbine drive system. The main purpose is to increase energy conversion efficiency and to reduce mechanical stress of the wind turbine. The control system performance is analyzed for MOD-2 wind turbine system.

Keywords: Wind Energy, Modeling, H_2 Control.

1. INTRODUCTION

The simplest configuration of a wind energy conversion system uses a stall-regulated wind turbine, where the power is naturally limited by aerodynamic efficiency decreasing due to stall effect (Novak et al., 1995). The turbine speed may be maintained constant when the generator is directly connected to the fixed-frequency utility grid, but, in this case, it is not possible to control the amount of power delivery by turbine to the generator. However, efficiency, mechanical stress and noise questions are better solved through variable speed operation. In this case, the generator is associated with power electronic converters, allowing power regulation by speed turbine adjustment (Novak et al., 1995).

Since wind system characteristics are highly dependent of wind speed, the quality of its control depends upon the stochastic properties of the controller. In this case, where disturbance rejection and noise suppression are important, the H_2 philosophy is particularly appropriate to controller design, offering robustness both to disturbances and system uncertainties (Grimble, 1994; Rocha et al., 1999).

In this paper, a linearized mathematical model of stall-regulated wind turbine is proposed and used to design an H_2 controller. A control strategy is proposed to increase the wind energy extract for variable speed operation. The control purposes are to attenuate torsional modes and to avoid fortuitous instabilities caused from wind turbulence and phenomena just as wind shear and aerodynamic stall. The proposed control scheme is analyzed through of simulation of MOD-2 wind turbine-generator system.

2. WIND ENERGY CONVERSION SYSTEM MODEL

The basic wind turbine drive system is composed by a wind turbine coupled at an electrical generator, directly or through gearbox, which can be adequately represented by approximated 2-mass model shown in Fig. 1. Supposing gearbox as ideal, this mechanical system can be described by:

$$J_t\dot{\omega}_t + D_t\omega_t = Q_a - Q_m - D_{hg}\left(\omega_t - \omega_g\right) \tag{1}$$
$$J_g\dot{\omega}_g + D_g\omega_g = D_{hg}\left(\omega_t - \omega_g\right) + Q_m - Q_g \tag{2}$$
$$Q_m = K_{hg}\int \left(\omega_t - \omega_g\right) dt \tag{3}$$

where ω_t= turbine speed, ω_g= generator speed, J_t= turbine inertia, J_g= generator inertia, D_t= turbine damping, D_g= generator damping, D_{hg}= shaft damping, K_{hg}= shaft stiffness, Q_a= aerodynamic torque, Q_g= generator torque and Q_m= shaft torque.

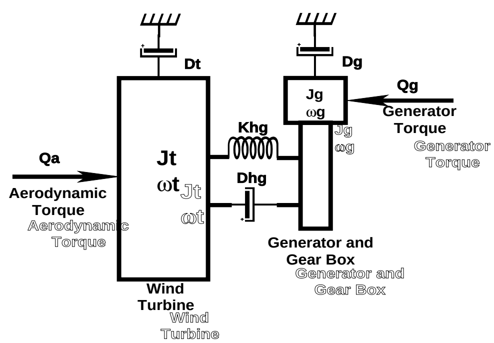

Figure 1: Wind turbine drive system model

The aerodynamic torque Q_a is better evaluated using dimensionless power coefficient C_p and torque coefficient C_q, which define the turbine ability to convert kinetic energy of moving air to mechanical power or torque (Novak et al., 1995):

$$Q_a = \frac{1}{2}\rho SR\frac{C_p}{\lambda}V^2 = \frac{1}{2}\rho SRC_qV^2 \tag{4}$$

where ρ= air density, S= rotor area, R= turbine radius, V= wind speed and λ is a parameter known as tip-speed ratio, defined as:

$$\lambda = \frac{R\omega_t}{V} \tag{5}$$

Both coefficients C_p e C_q are nonlinear functions of tip-speed ratio λ as shown in Fig. 2. It is possible to identify two distinct regions in turbine operation. The region "A" is stable and characterized by a negative slope, corresponding to normal region of turbine operation. The region "B" corresponds to aerodynamic stall, where aerodynamic torque

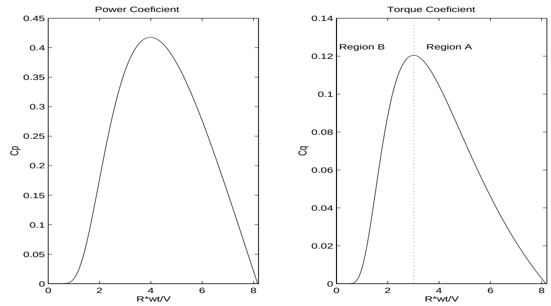

Figure 2: $C_p(\lambda)$ and $C_q(\lambda)$ of MOD-2 wind turbine

drops suddenly. This region is unstable and characterized by a positive slope. For control design, a linearized aerodynamic torque in region "A" can be used in modelling without degeneration of results (Novak et al., 1995; Rocha et al., 1999). The time derivative of aerodynamic torque Q_a for maximum C_p is:

$$\dot{Q}_a = \alpha \dot{V} + \gamma \dot{\omega}_t \tag{6}$$

where α and γ can be easily calculated from wind turbine data by:

$$\alpha = \left.\frac{\delta Q_a}{\delta V}\right|_{opt} = \frac{1}{2}\rho A R C_{pmax}\left(2\frac{V}{\lambda_{opt}} - 1\right) \tag{7}$$

$$\gamma = \left.\frac{\delta Q_a}{\delta \omega_t}\right|_{opt} = -\frac{1}{2}\rho A R^3 \frac{C_{pmax}}{\lambda_{opt}^2} \tag{8}$$

The electrical generator is the link between mechanical energy and electricity. It can be connected to electrical load directly or through electronic devices used to process the generated electrical energy. In last case, the generator torque is virtually independent of system dynamics (Novak et al., 1995), and its adjustment provides a way to regulate turbine speed and system efficiency, consisting in only manner to control a stall-regulated wind turbine. From equations (1), (2), (3) and (6), a linearized state model for stall-regulated wind turbine can be given by:

$$\dot{\mathbf{x}} = \mathbf{A}\mathbf{x} + \mathbf{b}u + \boldsymbol{\xi} \tag{9}$$

$$\mathbf{y} = \mathbf{c}\mathbf{x} + \eta \tag{10}$$

where $\mathbf{x}^T = \begin{bmatrix} Q_a & \omega_t & \omega_g & Q_m \end{bmatrix}$, $\mathbf{u} = Q_g$ and $\boldsymbol{\xi}^T = \begin{bmatrix} \alpha\dot{V} & 0 & 0 & 0 \end{bmatrix}$. The vector $\boldsymbol{\xi}$ is the disturbance on aerodynamic torque due to wind speed fluctuation $\dot{V}$, which can be assumed as white noise with zero mean in steady state (Wasynczuk et al., 1981). The measurement noise is represented by η and matrices $\mathbf{A}, \mathbf{b}$ and $\mathbf{c}$ are given by:

$$\mathbf{A} = \begin{bmatrix} \gamma\frac{1}{J_t} & -\gamma\frac{D_t+D_{hg}}{J_t} & \gamma\frac{D_{hg}}{J_t} & -\gamma\frac{1}{J_t} \\ \frac{1}{J_t} & -\frac{D_t+D_{hg}}{J_t} & \frac{D_{hg}}{J_t} & -\frac{1}{J_t} \\ 0 & \frac{D_{hg}}{J_g} & -\frac{D_{hg}+D_g}{J_g} & \frac{1}{J_g} \\ 0 & K_{hg} & -K_{hg} & 0 \end{bmatrix}, \quad \mathbf{b} = \begin{bmatrix} 0 \\ 0 \\ -\frac{1}{J_g} \\ 0 \end{bmatrix}, \quad \mathbf{c} = \begin{bmatrix} 0 & 0 & 1 & 0 \end{bmatrix}$$

3. H_2 TECHNIQUE

A feedback control design consists essentially in to find a controller K which assures stability, performance and robustness requirements, minimizing sensitivity S and complementary sensitivity T functions. However, it is not possible to minimize simultaneously

S and T, since that (Safonov et al., 1981):

$$S(s) + T(s) = I \tag{11}$$

Then, a compromise must be established between stability, performance and robustness requirements, favoring sensitivity S or complementary sensitivity T in accordance with relative importance of disturbance/reference and uncertainties power at each frequency (Safonov et al., 1981; Stein & Athans, 1987).

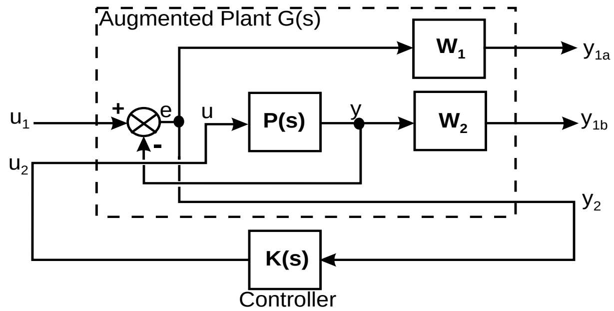

Figure 3: Plant Augmentation

This control problem can be formalized as H_2 optimization problem to find a controller K which stabilizes internally the augmented system of figure 3, given by:

$$P(s) = \left[\begin{array}{c|cc} A & B_1 & B_2 \\ \hline C_1 & D_{11} & D_{12} \\ C_2 & D_{21} & D_{22} \end{array}\right] \tag{12}$$

so that H_2 norm of transfer matrix between outlet and noise is minimized. This optimization problem is equivalent to conventional problem LQG (Grimble, 1994; Stein & Athans, 1987), involving a cost function:

$$J = \lim_{T\to\infty} E\left\{\int_0^T \left[\begin{array}{cc} x^T & u_2^T \end{array}\right] \left[\begin{array}{c} C_1^T \\ D_{12}^T \end{array}\right] \left[\begin{array}{cc} C_1 & D_{12} \end{array}\right] \left[\begin{array}{c} x^T \\ u_2^T \end{array}\right]\right\} \tag{13}$$

with correlated white plant noise ξ and white measurement η entering the system via the channel $\left[\begin{array}{cc} B_1 & D_{21} \end{array}\right]$ associated with correlation function:

$$E\left\{\left[\begin{array}{c} \xi(t) \\ \eta(\tau) \end{array}\right] \left[\begin{array}{cc} \xi^T(t) & \eta^T(\tau) \end{array}\right]\right\} = \left[\begin{array}{cc} B_1B_1^T & B_1D_{12}^T \\ D_{12}B_1^T & D_{12}D_{12}^T \end{array}\right]^T \delta(t-\tau) \tag{14}$$

In this way, The H_2 optimal controller K is realizable through of resolution of two Riccatti equations to find a full-state feedback K_c and a Kalman filter with residual gain matrix K_f.

4. CONTROL DESIGN

The turbine speed is the most important variable on wind turbine control, mainly for stall-regulated wind turbines. To obtain the maximum efficiency on energy conversion in subnominal speed range, the wind system must operate at constant tip-speed ratio λ to maintain the maximum C_p. The block diagram of proposed control strategy is shown in Fig. 4.

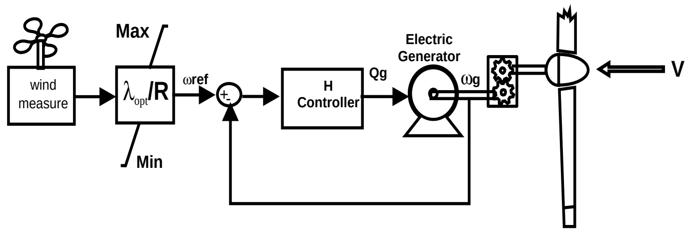

Figure 4: Control block diagram

Due to direct dependence of speed reference with wind speed in this control strategy, sudden variations of wind speed can excite torsional modes, inducing unacceptable mechanical stress in wind turbine. Thus, the design control specification must assure a good attenuation for torsional modes, as well to harmonic frequencies introduced by wind fluctuation and other aerodynamic force sources as wind shear and stall effect. It is necessary to avoid the operation in stall region to assure better performance of wind energy conversion system.

The aerodynamic behavior of the wind turbine is nonlinear, dependent on wind speed and may change over time due to contamination of blade surfaces. Because of complexity of the interaction of the rotor with wind-field, it is not possible to quantify the uncertainty in the aerodynamic models. However, according to (Leith & Leithead, 1997), practical experience indicates that 10 dB is an appropriate gain margin and roughly 60 degrees the appropriate phase margin. The close loop poles have to be placed as far away as possible from frequencies of large amounts of fluctuation energy in the wind and other sources of force to avoid instabilities in system operation.

5. SIMULATION RESULTS

The performance of the purposed H_2 controller was simulated using the MOD-2 wind turbine-generator system complete model given by (Wasynczuk et al., 1981), which data are shown in table 1. The weighting functions $W_1(s)$ and $W_2(s)$ are selected as:

$$W_1(s) = 40\frac{s+1.1}{(s+\epsilon)(1.1s+1)} \tag{15}$$

$$W_2(s) = \frac{(s+2.5)^2}{s+1500} \tag{16}$$

Table 1: MOD-2 system data referred to a 2.5 MVA base and 1.84 rad/sec

J_t	D_t	J_g	D_g	K_{hg}	D_{hg}
$37,413$	$2,024\times10^{-2}$	$2,091$	$3,01\times10^{-2}$	$28,4$	$1,831$

The integral action is incorporated in weighting $W_1(s)$ with the inclusion of term $1/(s+\epsilon)$, where ϵ is a very small variable, aiming to achieve a zero steady-state error and disturbance reduction. The Bode diagrams for close-loop system shows cross-over frequency around 20 rad/s, gain margin about 10 dB and phase margin as 61 degrees, which assures the robustness design specifications. The dynamic behavior of this controlled MOD-2 system when submitted at wind fluctuation and a step on wind speed are shown respectively in Figs. 5 and 6. In both simulations, the aerodynamic torque Q_a is corrupted with ripple torque due to aerodynamic forces sources just as wind shear, tower shadow, stall phenomenon, etc.

The generator speed control was relatively accurate as shown in figures 5.b and 6.b. Since speed reference is directly dependent of wind speed, a noise is added to the system due to wind fluctuation that reduces the system lifetime. Thus, it is necessary to filter the speed reference signal, although sometimes this function is performed by anemometer inertia. From figures 5.c and 6.c, it is noted that electrical torque Q_g tend to oppose the aerodynamic torque Q_a, providing a fast speed adjustment and better ripples attenuation. The system operates around optimal tip-speed ratio as shown in 5.d and 6.d, assuring good efficiency for wind energy conversion system.

6. CONCLUSION

A simplified wind system model is proposed and considerations for energy conversion efficiency maximization and mechanical stress reduction are presented. A speed controller for the wind system is designed using H_2 technique to assure control requirements. The control system performance is verified through of simulation of MOD-2 wind turbine-generator system. The simulation results show good H_2 performance, since the wind energy conversion system operated near optimal tip-speed ratio even with wind speed disturbances with a good ripple torque attenuation.

7. REFERENCES

Grimble, M. J., 1994, Robust industrial control - Optimal design approach for polynomial system, Prentice Hall International, New York, USA.

Leith, D. J., & Leithead, W., 1997, Implementation of wind turbine controllers, Technical Report, Department of Electronic & Electrical Engineering, University of Strathclyde, Glasgow, UK.

Novak, P., Ekelund, T., Jovik, I. & Schmidtbauer, B., 1995, Modeling and control of variable-speed wind-turbine drive-system dynamics, IEEE Control Systems, vol. 15, n. 4, pp. 28-38.

Rocha, R., Resende, P., Silvino, J. L. & Bortolus, M. V., 1999, Modeling and LQG/LTR discrete control of a wind energy conversion system, 15th Brazilian Congress of Mechanical Engineering, Águas de Lindóia, Brazil.

Safonov, M. G., Laub, A. J. & Hartmann, G. L., 1981, Feedback properties of multivariable systems: the role and use of the return difference matrix, IEEE Trans. on Automatic Control,vol. 26, n. 1, pp. 47-65.

Stein, G. & Athans, M., 1987, The LQG/LTR procedure for multivariable feedback control design, IEEE trans. on Automatic Control, vol 32, n. 2, pp. 105-114.

Wasynczuk, O., Man, D. T. & Sullivan, J. P., 1981, Dynamic behaviour od a class of wind turbine generators during random wind fluctuations, IEEE trans. on Power Apparatus and Systems, vol. 100, n. 6, pp 2837-2845.

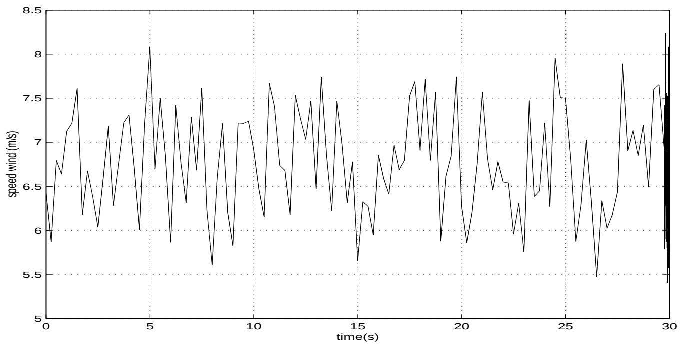

(a) Wind speed

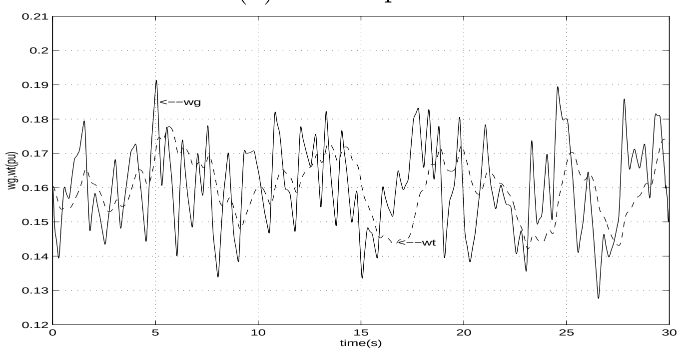

(b) Generator and wind turbine speeds

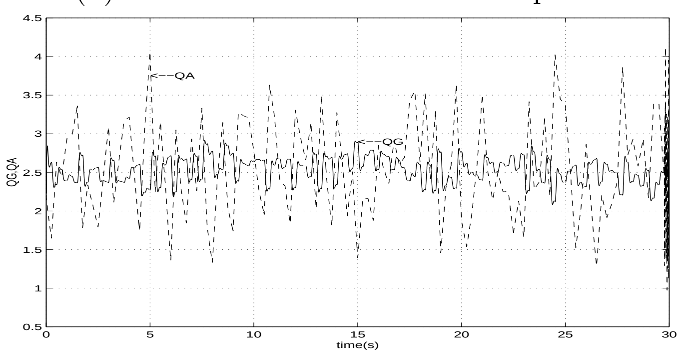

(c) Aerodynamic and generator torques

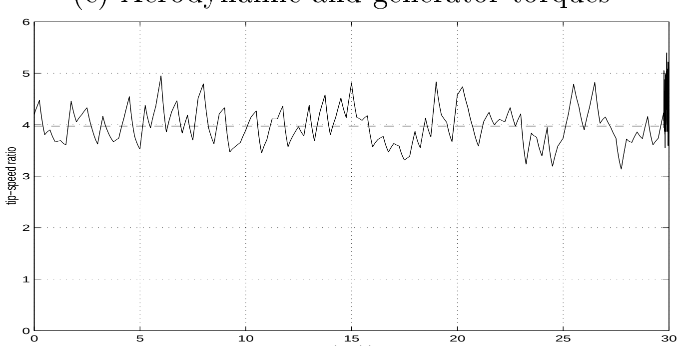

(d) Tip-speed ratio

Figure 5: System behaviour with wind fluctuation

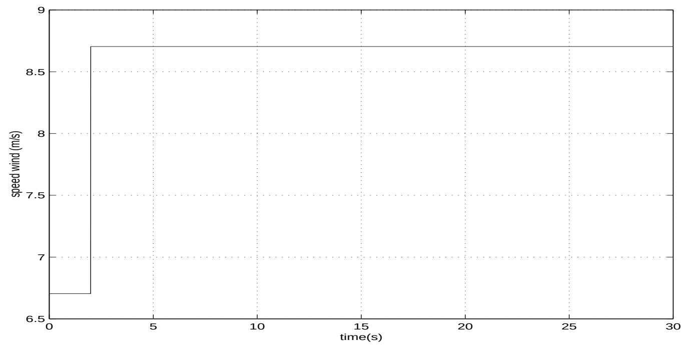

(a) Wind speed

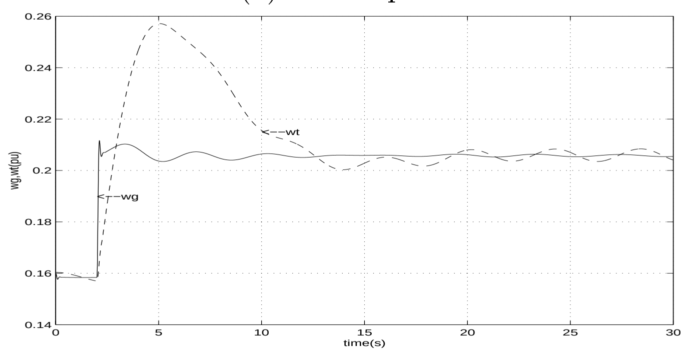

(b) Generator and turbine speeds

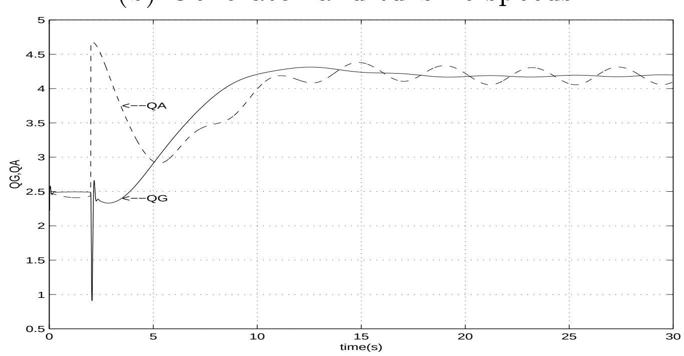

(c) Aerodynamic and generator torques

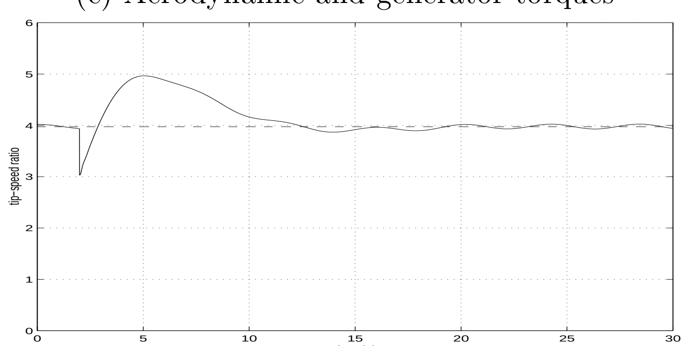

(d) Tip-speed ratio

Figure 6: System behaviour with step on speed wind